ISSN 0020-1685, Inorganic Materials, 2007, Vol. 43, No. 11, pp. 1252–1257. © Pleiades Publishing, Inc., 2007.
Original Russian Text © S.A. Solopan, O.I. V'yunov, A.I. Tovstolytkin, L.L. Kovalenko, A.G. Belous, 2007, published in Neorganicheskie Materialy, 2007, Vol. 43, No. 11, pp. 1389–1395.

Substrate Effect on the Properties of $La_{0.775}Sr_{0.225}MnO_3$ Films

S. A. Solopan[a], O. I. V'yunov[a], A. I. Tovstolytkin[b], L. L. Kovalenko[a], and A. G. Belous[a]

[a] *Vernadsky Institute of General and Inorganic Chemistry, National Academy of Sciences of Ukraine, pr. Akademika Palladina 32/34, Kiev, 03680 Ukraine*

[b] *Institute of Magnetism, National Academy of Sciences of Ukraine, bul'v. Akademika Vernadskogo 36b, Kiev, 03142 Ukraine*

e-mail: vyunov@ionc.kar.net

Received November 9, 2006

Abstract—$La_{0.775}Sr_{0.225}MnO_3$ films have been produced by screen printing on various substrates (Al_2O_3, $BaTi_{0.85}Zr_{0.11}Sn_{0.04}O_3$, $Ba_{0.996}Y_{0.004}TiO_3$, $Ba_{0.996}Y_{0.004}TiO_3$ + 0.04%Mn, and $Ba_{0.996}Y_{0.004}Ti_{0.65}Sn_{0.35}O_3$), and their electrical properties have been studied in comparison with those of bulk materials. The structural properties of the substrates are shown to influence the electrical properties of the films.

DOI: 10.1134/S0020168507110167

INTRODUCTION

There is wide research interest in $La_{1-x}M_xMnO_3$ (M = alkaline-earth metal) doped lanthanum manganites with a distorted perovskite structure, which exhibit a colossal magnetoresistive response and possess a unique combination of structural, electrical, and magnetic properties [1, 2]. The magnetic and electrical properties of these materials are very sensitive to their microstructure (grain size, porosity, etc.) and also to whether the material is in bulk or thin-film form [3]. The first syntheses of bulk materials and their electrical properties were reported in [4–6]. The properties of magnetic films were first described by Chahara et al. [7]. Manganite films can be prepared by a number of techniques: magnetron sputtering [8], pulsed laser deposition [9], pulsed injection metalorganic chemical vapor deposition [10], and sol–gel processing [11]. A systematic analysis of the literature shows that the microstructure and electrical properties of manganite films strongly depend on the nature of the substrate [12]. Moreover, manganite films may exhibit a stronger magnetoresistive effect in comparison with bulk materials [13].

In recent years, considerable interest has been centered on multilayer structures combining the properties of magnetic films and substrates [14]. The ability to fabricate such structures would made it possible to create novel types of devices in which the properties of one material could be controlled by varying the properties of the other.

In this paper, we describe the synthesis, structure, and magnetoresistive response of $La_{0.775}Sr_{0.225}MnO_3$ films produced by screen printing on substrates of α-Al_2O_3 and barium-titanate-based ceramics, whose properties can be controlled by applying an electric field.

EXPERIMENTAL

To produce $La_{0.775}Sr_{0.225}MnO_3$ films by screen printing, we first prepared fine powder of this composition by solid-state reaction. The powder was then ground and dispersed by sonication with a UZDN-2T processor. Next, we prepared a homogeneous colloidal solution of the synthesized powder using ethylene glycol as a solvent. The $La_{0.775}Sr_{0.225}MnO_3$ films were applied to 200-μm-thick substrates by screen printing [15], followed by heat treatment at 1440 K for 2 h. The substrates used were of barium-titanate-based ceramics which possessed ferroelectric, semiconducting, and nonlinear dielectric properties. The $BaTi_{0.85}Zr_{0.11}Sn_{0.04}O_3$ material has nonlinear properties (nonlinear variation of dielectric permittivity with the applied electric filed) [16]. Materials based on $Ba_{0.996}Y_{0.004}TiO_3$, $Ba_{0.996}Y_{0.004}TiO_3$ + 0.04%Mn, and $Ba_{0.996}Y_{0.004}Ti_{0.65}Sn_{0.35}O_3$ are ferroelectric semiconductors (have a positive temperature coefficient of resistance) and differ in room-temperature resistivity and phase-transition temperature [17]. As a control substrate, we used α-Al_2O_3, a nonconductive material which does not have nonlinear properties.

X-ray diffraction (XRD) measurements were performed on a DRON-4-07 powder diffractometer (CuK_α radiation, $2\theta = 10°–150°$). Structural parameters were refined by the Rietveld profile analysis method. The thickness of the films was determined by scanning electron microscopy (SEM) on a JEOL JCXA-733 Super-Probe. The electrical resistance of the films was mea-

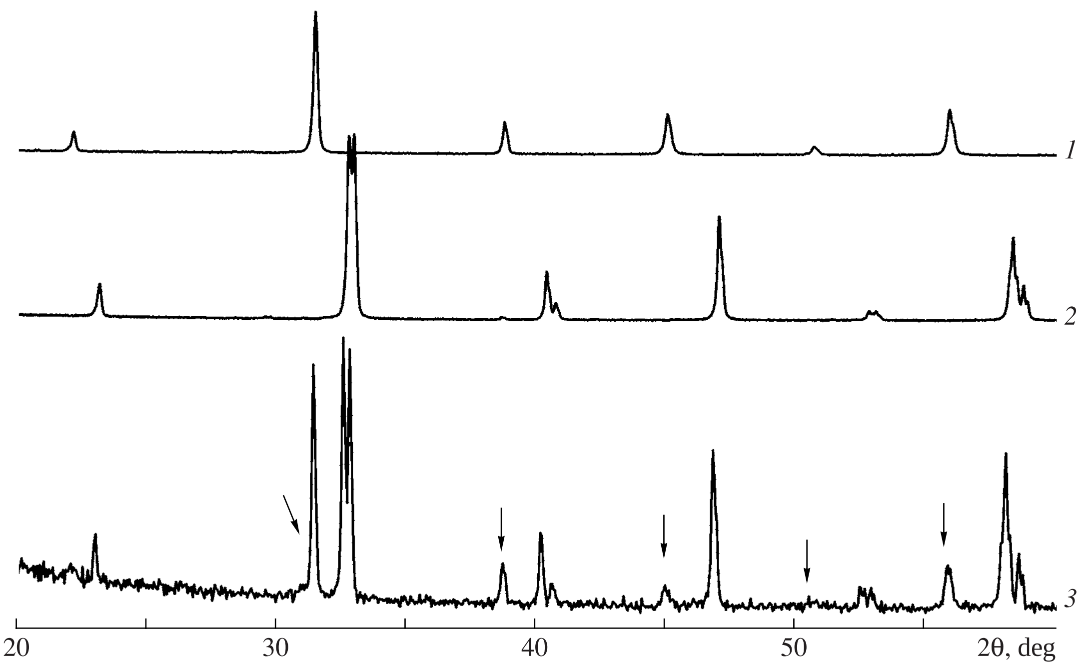

Fig. 1. XRD patterns of (*1*) bulk $BaTi_{0.85}Zr_{0.11}Sn_{0.04}O_3$, (*2*) bulk $La_{0.775}Sr_{0.225}MnO_3$, and (*3*) an $La_{0.775}Sr_{0.225}MnO_3$ film on a $BaTi_{0.85}Zr_{0.11}Sn_{0.04}O_3$ substrate; the arrows mark peaks from the substrate.

sured by a four-probe technique from 77 to 350 K. Silver contacts were deposited by magnetron sputtering. Magnetoresistance (MR), $(R_0 - R_H)/R_0 \times 100\%$, where R_0 is the zero-field resistance, and R_H is the resistance in magnetic field H, was determined in applied fields of up to 1.2 MA/m.

RESULTS AND DISCUSSION

XRD examination showed that the $La_{0.775}Sr_{0.225}MnO_3$ samples used to produce films were single-phase and had a rhombohedrally distorted perovskite structure, sp. gr. $R\bar{3}c$. The substrate materials for manganite film deposition were also single-phase and had a tetragonal perovskite structure, sp. gr. $P4mm$ ($BaTi_{0.85}Zr_{0.11}Sn_{0.04}O_3$, $Ba_{0.996}Y_{0.004}TiO_3$, $Ba_{0.996}Y_{0.004}TiO_3$ + 0.04%Mn $Ba_{0.996}Y_{0.004}Ti_{0.65}Sn_{0.35}O_3$) or a rhombohedral structure, sp. gr. $R\bar{3}c$ (Al_2O_3).

The XRD patterns of our samples (Fig. 1) showed that the $La_{0.775}Sr_{0.225}MnO_3$ films produced on various substrates were single-phase and differed in lattice orientation. Curve *1* in Fig. 2 represents an XRD scan of bulk $La_{0.775}Sr_{0.225}MnO_3$. The 110 and 104 reflections are seen to be close in intensity, in accordance with calculation. The $La_{0.775}Sr_{0.225}MnO_3$ films on Al_2O_3 and $Ba_{0.996}Y_{0.004}Ti_{0.65}Sn_{0.35}O_3$ substrates (scans *2*, *3*) are [001]-oriented, which increases the intensity of the 104 reflection. As seen in Fig. 2, in the other systems (scans *4–6*) the 110 reflection is stronger, indicating (110) preferential alignment. It is well known that the texturing factor may attest to preferential orientation ($G \neq 0$, $G \neq 1$) or to an orientation-disordered state ($G = 0$, $G = 1$) [18].

Tables 1 and 2 list the Rietveld-refined structural parameters of bulk samples and screen-printed films. To obtain accurate data, the refinement included the parameters of both the film and substrate. It can be seen that the structural parameters of the substrate influence both the preferential orientation and structural parameters of the film. Reducing the structural parameters of the substrate reduces those of the films. This can be accounted for by the film crystallization in the direction of the orientation of the substrate surface.

The thickness of the films was determined by SEM (Fig. 3). The results indicate that all of the films are $\simeq$100 μm in thickness.

Figure 4 shows the temperature dependences of normalized resistance for bulk samples and films of $La_{0.775}Sr_{0.225}MnO_3$ on various substrates. The peak-resistance temperature T_{max} of the film on the alumina substrate (curve *2*) is lower than that of bulk $La_{0.775}Sr_{0.225}MnO_3$ (curve *1*). At the same time, the maximum in the resistance of the films on the $BaTi_{0.85}Zr_{0.11}Sn_{0.04}O_3$, $Ba_{0.996}Y_{0.004}TiO_3$ + 0.04% Mn, and $Ba_{0.996}Y_{0.004}Ti_{0.65}Sn_{0.35}O_3$ substrates is shifted to higher temperatures in comparison with the ceramic sample (curves *3–5*). This effect can be understood in terms of the preferential orientation of the films relative to the substrate [19]. Moreover, the resistance of the films is influenced by the characteristics of the parti-

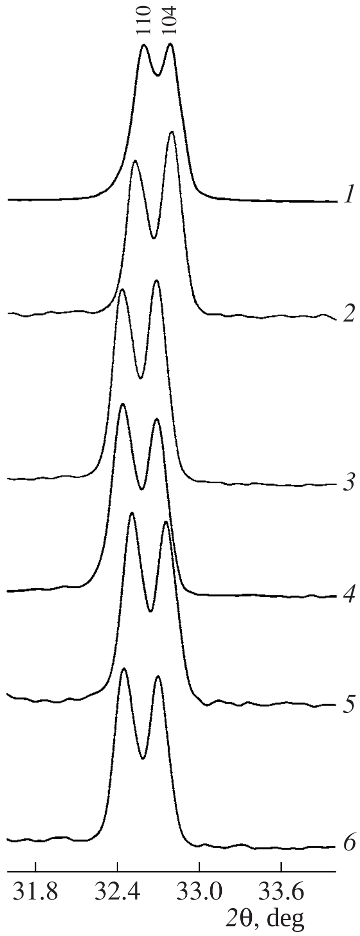

Fig. 2. XRD scans of $La_{0.775}Sr_{0.225}MnO_3$: bulk sample (*1*) and films produced on α-Al_2O_3 (*2*), $Ba_{0.996}Y_{0.004}Ti_{0.65}Sn_{0.35}O_3$ (*3*), $Ba_{0.996}Y_{0.004}TiO_3$ + 0.04% Mn (*4*), $BaTi_{0.85}Zr_{0.11}Sn_{0.04}O_3$ (*5*), and $Ba_{0.996}Y_{0.004}TiO_3$ (*6*).

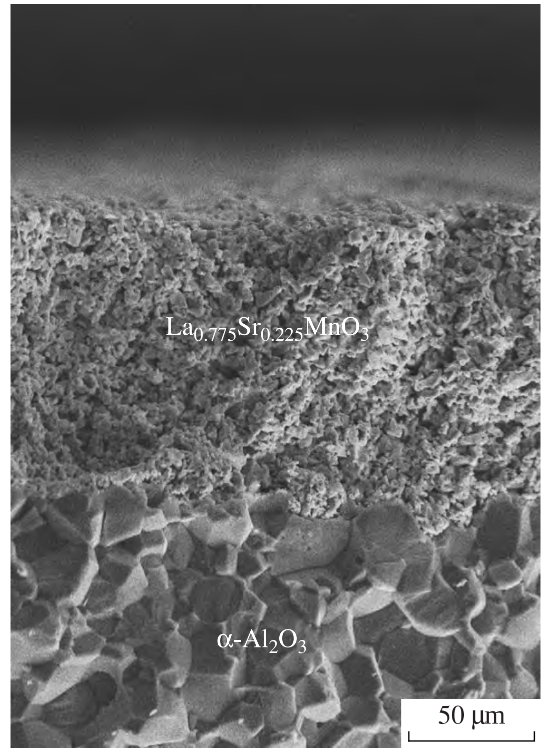

Fig. 3. SEM micrograph of the $La_{0.775}Sr_{0.225}MnO_3$ film on α-Al_2O_3.

cles, in particular by their structural and magnetic disorder, and also by deviations of the chemical composition from the nominal one at grain boundaries [20]. It should also be taken into account that the inhomogeneous elastic strain in manganite films increases the scatter in the effective manganese–oxygen bond length, which also contributes to changes in T_{max} [13, 14].

Figure 5 shows the temperature dependences of magnetoresistance in an applied field H = 1.2 MA/m for polycrystalline and thin-film $La_{0.775}Sr_{0.225}MnO_3$ samples. According to earlier results [21, 22], the magnetoresistance of single-crystal manganites has a maximum near their Curie temperature T_C (metallic ferromagnet–dielectric paramagnet transition). In polycrystalline samples, there is an additional contribution to MR at low temperatures ($T < T_C$), which rises steadily with decreasing temperature. This contribution was attributed to spin-dependent grain-boundary scattering of charge carriers [21] or to spin-polarized grain-boundary tunneling [20]. Both in bulk

Table 1. Unit-cell parameters of bulk samples

Composition	Sp. gr.	*Z*	*a*, Å	*c*, Å	*V*, Å^3	*G* [*hkl*]
$La_{0.775}Sr_{0.225}MnO_3$	$R\bar{3}c$	6	5.502(4)	13.349(6)	350.0(4)	0
Al_2O_3	$R\bar{3}c$	6	4.754(1)	12.982(1)	254.1(1)	1.61 [001]
$Ba_{0.996}Y_{0.004}TiO_3$ + 0.04%Mn	*P4mm*	1	3.9940(8)	4.029(1)	64.28(2)	0.38 [110]
$Ba_{0.996}Y_{0.004}TiO_3$	*P4mm*	1	3.9969(2)	4.0341(3)	64.448(8)	1.17 [110]
$BaTi_{0.85}Zr_{0.11}Sn_{0.04}O_3$	*P4mm*	1	4.0304(2)	4.0368(3)	65.576(6)	0.95 [110]
$Ba_{0.996}Y_{0.004}Ti_{0.65}Sn_{0.35}O_3$	*P4mm*	1	4.0418(6)	4.0516(7)	66.19(1)	0.23 [001]

Table 2. Unit-cell parameters of $La_{0.775}Sr_{0.225}MnO_3$ films on different substrates

Substrate composition	*a*, Å	*c*, Å	*V*, Å^3	*G* [*hkl*]
Al_2O_3	5.5223(6)	13.372(1)	353.16(7)	0.15 [001]
$Ba_{0.996}Y_{0.004}TiO_3$ + 0.04%Mn	5.5227(1)	13.3700(2)	353.162(9)	0.04 [110]
$Ba_{0.996}Y_{0.004}TiO_3$	5.5195(1)	13.3654(4)	352.63(1)	0.14 [110]
$BaTi_{0.85}Zr_{0.11}Sn_{0.04}O_3$	5.5208(2)	13.3679(7)	352.86(2)	0.11 [110]
$Ba_{0.996}Y_{0.004}Ti_{0.65}Sn_{0.35}O_3$	5.5236(2)	13.3770(7)	353.45(3)	0.03 [001]

$La_{0.775}Sr_{0.225}MnO_3$ and in the films on doped barium titanate substrates, the two contributions to magnetoresistance are significant (Fig. 5), which allows the T_C of these samples to be evaluated as the peak temperature in the MR(T) curve. The temperature variation of MR for the film on the alumina substrate is typical of materials with a diffuse phase transition (inhomogeneous or strained manganites) [14]. Thus, the present results demonstrate that the films produced on alumina and doped barium titanate substrates differ in transition temperature, which is no doubt associated with the difference in the preferential orientation of the films relative to the substrate [23].

Dorr [14] discussed the potential of composite films such as substituted lanthanum manganite/doped barium titanate for use in devices whose magnetic or magnetoresistive properties can be tuned by an applied electric field. The proposed mechanisms of magnetoelectric coupling include the inverse piezoelectric effect and the formation of an excess charge at the film/substrate interface [14]. To ascertain whether such effects do take place in our structures, we studied the electric-field effect on the properties of doped lanthanum manganite films.

Figure 6 schematically illustrates the film–substrate geometry we used to study the influence of the nonlinear properties of $BaTi_{0.85}Zr_{0.11}Sn_{0.04}O_3$ substrates and the ferroelectric–semiconducting properties of $Ba_{0.996}Y_{0.004}TiO_3$, $Ba_{0.996}Y_{0.004}TiO_3$ + 0.04% Mn, and $Ba_{0.996}Y_{0.004}Ti_{0.65}Sn_{0.35}O_3$ substrates on the properties of manganite films. The electrical resistance and magnetoresistance of the films was determined using electrodes *4* and *5*. The measurements were made in an applied magnetic and/or electric field or in zero field. As an example, Fig. 7 shows the temperature dependences of electrical resistance for an $La_{0.775}Sr_{0.225}MnO_3$ film on a $Ba_{0.996}Y_{0.004}TiO_3$ + 0.04% Mn substrate in different applied electric fields. At zero voltage or a voltage applied between electrodes *2* and *3*, the slope of the $R(T)$ curve changes sharply near the phase transition (curves *2*, *3*). A voltage applied between electrodes *1* and *2* (curve *1*) shifts the phase transition and reduces the resistance of the film. This behavior can be

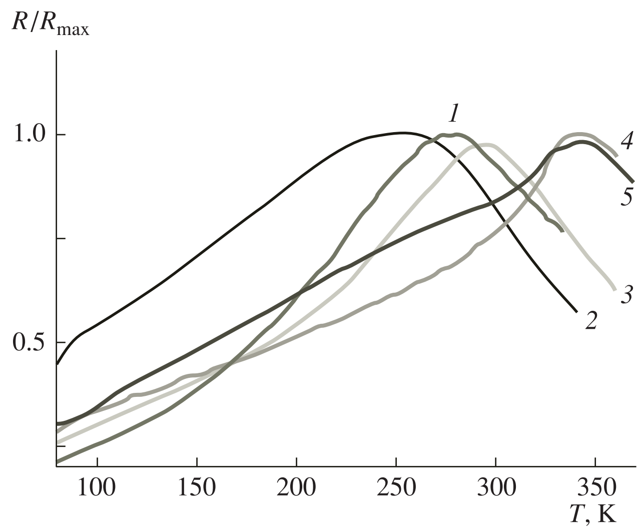

Fig. 4. Temperature dependences of normalized resistance for a bulk $La_{0.775}Sr_{0.225}MnO_3$ sample (*1*) and $La_{0.775}Sr_{0.225}MnO_3$ films on α-Al_2O_3 (*2*), $Ba_{0.996}Y_{0.004}Ti_{0.65}Sn_{0.35}O_3$ (*3*), $BaTi_{0.85}Zr_{0.11}Sn_{0.04}O_3$ (*4*), and $Ba_{0.996}Y_{0.004}TiO_3$ + 0.04% Mn (*5*).

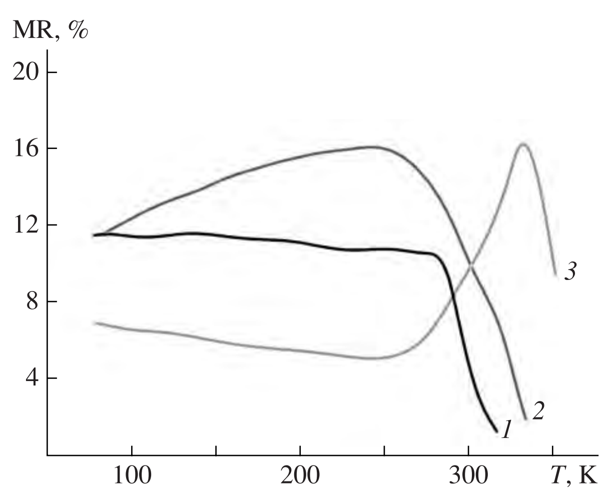

Fig. 5. Temperature dependences of magnetoresistance for a bulk $La_{0.775}Sr_{0.225}MnO_3$ sample (*1*) and $La_{0.775}Sr_{0.225}MnO_3$ films on α-Al_2O_3 (*2*) and $BaTi_{0.85}Zr_{0.11}Sn_{0.04}O_3$ (*3*).

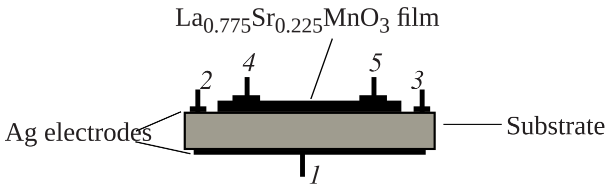

Fig. 6. Geometry of $La_{0.775}Sr_{0.225}MnO_3$ films on various substrates: (*1–3*) electrodes to the substrate, (*4*, *5*) electrodes to the film.

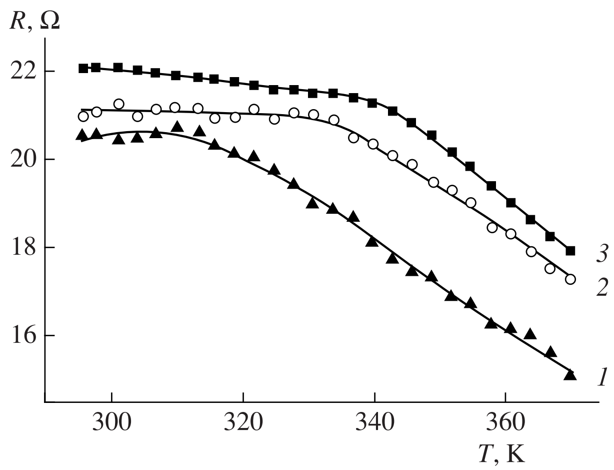

Fig. 7. Resistance as a function of temperature for an $La_{0.775}Sr_{0.225}MnO_3$ film on a $Ba_{0.996}Y_{0.004}TiO_3$ + 0.04% Mn substrate at a 30-V voltage applied (*1*) between electrodes *1* and *2* and (*2*) between electrodes *2* and *3*; (*3*) zero voltage.

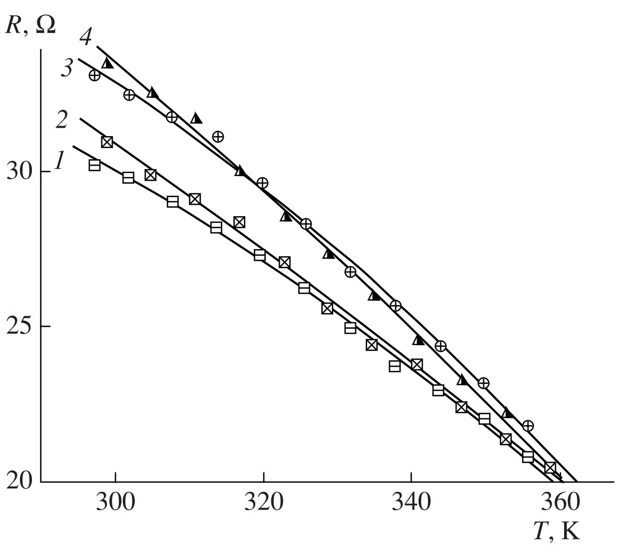

Fig. 8. Resistance as a function of temperature for an $La_{0.775}Sr_{0.225}MnO_3$ film on a $Ba_{0.996}Y_{0.004}Ti_{0.65}Sn_{0.35}O_3$ substrate in applied electric and magnetic fields: (*1*) H = 1.2 MA/m, V = 0; (*2*) H = 1.2 MA/m, V = 20 V between electrodes *1* and *2*; (*3*) H = 0, V = 0; (*4*) H = 0, V = 20 V between electrodes *1* and *2*.

accounted for by the sensitivity of the doped barium titanate to an external electric field and by the magnetoelectric coupling between the layers via the mechanisms described above. The shift of the phase transition in the manganite film (curve *1*) seems to be due to the higher electric field applied to the substrate: $E = V/d$, where d is the electrode separation.

Figure 8 shows the temperature dependences of resistance for an $La_{0.775}Sr_{0.225}MnO_3$ film on a $Ba_{0.996}Y_{0.004}Ti_{0.65}Sn_{0.35}O_3$ substrate in applied electric and magnetic fields. An electric field applied to the substrate is seen to have little effect on the resistance of the film, whereas an applied magnetic field reduces it (curves *1*, *2*), which is characteristic of manganites [13, 14]. The weaker electric-field effect on the properties of the system substituted lanthanum manganite–doped barium titanate seems to be associated with the weaker sensitivity of the properties of $Ba_{0.996}Y_{0.004}Ti_{0.65}Sn_{0.35}O_3$ to electric fields.

CONCLUSIONS

The present results demonstrate that screen printing is a viable approach for the preparation of $La_{0.775}Sr_{0.225}MnO_3$ manganite films on ceramic substrates of various compositions. The lattice parameters and preferential orientation of substrates are shown to influence the lattice parameters of the films, which, in turn, leads to changes in their electrical properties and magnetoresistive response. The use of $BaTi_{0.85}Zr_{0.11}Sn_{0.04}O_3$, $Ba_{0.996}Y_{0.004}TiO_3$, $Ba_{0.996}Y_{0.004}TiO_3$ + 0.04%Mn, and $Ba_{0.996}Y_{0.004}Ti_{0.65}Sn_{0.35}O_3$ substrates makes it possible to raise the phase transition temperature of manganite films. An appropriate choice of substrate composition enables the synthesis of substituted lanthanum manganite/doped barium titanate structures, whose magnetoresistive properties can be tuned by applying an electric field.

REFERENCES

1. Nagaev, E.L., Lanthanum Manganites and Other Colossal Magnetoresistance Magnetic Conductors, *Usp. Fiz. Nauk*, 1996, vol. 166, no. 8, pp. 833–858.
2. Nagai, T., Yamazaki, A.., Uehara, M., et al., Sintering of Non-stoichiometric$Nd_{1-x}MnO_{3-y}$ Powders Prepared by a Coprecipitation Method, *J. Mater. Sci. Lett.*, 2000, vol. 19, no. 20, pp. 1821–1823.
3. Wang, X.L., Dou, S.X., Liu, H.K., et al., Large Low-Field Magnetoresistance over a Wide Temperature Range Induced by Weak-Link Grain Boundaries in $La_{0.7}Ca_{0.3}MnO_3$, *App. Phys. Lett.*, 1998, vol. 73, no. 3, pp. 396–398.
4. Jonker, G.H. and Van Santen, J.H., Ferromagnetic Compounds of Manganese with Perovskite Structure, *Physica* (Amsterdam, Neth.), 1950, vol. 16, pp. 337–349.
5. Van Santen, J.H. and Jonker, G.H., Electrical Conductivity of Ferromagnetic Compounds of Manganese with

Perovskite Structure, *Physica* (Amsterdam, Neth.), 1950, vol. 16, pp. 599–600.

6. Volger, J., Further Experimental Investigations on Some Ferromagnetic Oxidic Compounds of Manganese with Perovskite Structure, *Physica* (Amsterdam, Neth.), 1954, vol. 20, pp. 49–66.
7. Chahara, K., Ohno, T., Kasai, M., and Kozono, Y., Magnetoresistance in Magnetic Manganese Oxide with Intrinsic Antiferromagnetic Spin Structure, *Appl. Phys. Lett.*, 1993, vol. 63, pp. 1990–1992.
8. Li, K., Qi, Z., Li, X., et al., Growth, Structural Characteristics, and Magnetoresistance in LaCaMnO Thin Films Prepared by dc Magnetron Sputtering, *Thin Solid Films*, 1997, vol. 304, pp. 386–391.
9. Jo, M.-H., Mathur, N.D., Evetts, J.E., and Blamire, M.G., Inhomogeneous Transport in Heteroepitaxial $La_{0.7}Ca_{0.3}MnO_3/SrTiO_3$ Multilayers, *Appl. Phys. Lett.*, 1999, vol. 75, pp. 3689–3691.
10. Rosina, M., Audier, M., Dubourdieu, C., et al., Defects in $(La_{0.7}Sr_{0.3}MnO_3/SrTiO_3)_{15}$ Superlattices Grown by Pulsed Injection MOCVD, *J. Cryst. Growth*, 2003, vol. 259, no. 4, pp. 358–366.
11. Venkataiah, G., Krishna, D.C., Vithal, M., et al., Effect of Sintering Temperature on Electrical Transport Properties of $La_{0.67}Ca_{0.33}MnO_3$, *Phys. B* (Amsterdam, Neth.), 2005, vol. 357, pp. 370–379.
12. Yang, S.Y., Kuang, W.L., Liou, Y., et al., Growth and Characterization of $La_{0.7}Sr_{0.3}MnO_3$ Films on Various Substrates, *J. Magn. Magn. Mater.*, 2004, vol. 268, no. 3, pp. 326–331.
13. Tovstolytkin, A.I., Pogorily, A.N., Matviyenko, A.I., et al., Discrete Deposition As a Powerful Tool to Govern Magnetoresistance of the Doped Manganite Films, *J. Appl. Phys.*, 2005, vol. 98, no. 043902, pp. 1–6.
14. Dorr, K., Ferromagnetic Manganites: Spin-Polarized Conduction versus Competing Interactions, *J. Phys. D: Appl. Phys.*, 2006, vol. 39, pp. 125–150.
15. Dutronc, P., Carbonne, B., M’enil, F., and Lucat, C., Influence of the Nature of the Screen-Printed Electrode Metal on the Transport Properties of Thick-Film Semiconductor Gas Sensors, *Sens. Actuators, B*, 1992, vol. 6, pp. 279–284.
16. Solopan, S.A., V’yunov, O.I., Kovalenko, L.L., and Belous, A.G., Synthesis and Properties of Ferroelectric–Magnetic Composite Structures, *Ukr. Khim. Zh.*, 2006, vol. 72, no. 1, pp. 28–31.
17. Belous, A.G., V’yunov, O.I., and Kovalenko, L.L., $(Ba,Y)(Ti,Zr,Sn)O_3$-Based PTCR Materials, *Ferroelectrics*, 2001, vol. 254, nos. 1–4, pp. 91–99.
18. Rodriguez-Carvajal, J., *An Introduction to the Program FullProf 2000*, Cedex, 2001, pp. 54–55.
19. Chen, Ch.-C. and de Lozanne, A., Electronic Transport Properties of (001)/(110) Oriented $La_{2/3}MnO_{3-\delta}$ Thin Films, *Appl. Phys. Lett.*, 1998, vol. 73, no. 26, pp. 3950–3952.
20. Gross, R., Alff, L., Büchner, B., et al., Physics of Grain Boundaries in the Colossal Magnetoresistance Manganites, *J. Magn. Magn. Mater.*, 2000, vol. 211, nos. 1–3, pp. 150–159.
21. Li, X.W., Gupta, A., Xiao, G., and Gong, G.Q., Low-Field Magnetoresistive Properties of Polycrystalline and Epitaxial Perovskite Manganite Films, *Appl. Phys. Lett.*, 1997, vol. 71, no. 8, p. 1124.
22. Ghosh, K., Ogale, S.B., Ramesh, R., et al., Transition-Element Doping Effects in $La_{0.7}Ca_{0.3}MnO_3$, *Phys. Rev. B: Condens. Matter Mater. Phys.*, 2000, vol. 59, no. 1, pp. 533–537.
23. Nath, T.K., Rao, R.A., Lavric, D., and Eom, C.B., Effect of Three-Dimensional Strain States on Magnetic Anisotropy of $La_{0.8}Ca_{0.2}MnO_3$ Epitaxial Thin Films, *Appl. Phys. Lett.*, 1999, vol. 74, no. 11, pp. 1615–1617.